JACS
JOURNAL OF THE AMERICAN CHEMICAL SOCIETY

Article

pubs.acs.org/JACS

Design and Mechanism of Tetrahydrothiophene-Based γ-Aminobutyric Acid Aminotransferase Inactivators

Hoang V. Le,[†] Dustin D. Hawker,[†] Rui Wu,[‡] Emma Doud,[§] Julia Widom,[†] Ruslan Sanishvili,[∥] Dali Liu,[‡] Neil L. Kelleher,[§] and Richard B. Silverman*,[†]

[†]Departments of Chemistry and Molecular Biosciences, Chemistry of Life Processes Institute, and the Center for Molecular Innovation and Drug Discovery, Northwestern University, Evanston, Illinois 60208, United States

[‡]Department of Chemistry and Biochemistry, Loyola University Chicago, Chicago, Illinois 60660, United States

[§]Departments of Chemistry and Molecular Biosciences and the Proteomics Center of Excellence, Northwestern University, Evanston, Illinois 60208, United States

[∥]X-ray Science Division, Advanced Photon Source, Argonne National Laboratory, Lemont, Illinois 60439, United States

Supporting Information

ABSTRACT: Low levels of γ-aminobutyric acid (GABA), one of two major neurotransmitters that regulate brain neuronal activity, are associated with many neurological disorders, such as epilepsy, Parkinson's disease, Alzheimer's disease, Huntington's disease, and cocaine addiction. One of the main methods to raise the GABA level in human brain is to use small molecules that cross the blood−brain barrier and inhibit the activity of γ-aminobutyric acid aminotransferase (GABA-AT), the enzyme that degrades GABA. We have designed a series of conformationally restricted tetrahydrothiophene-based GABA analogues with a properly positioned leaving group that could facilitate a ring-opening mechanism, leading to inactivation of GABA-AT. One compound in the series is 8 times more efficient an inactivator of GABA-AT than vigabatrin, the only FDA-approved inactivator of GABA-AT. Our mechanistic studies show that the compound inactivates GABA-AT by a new mechanism. The metabolite resulting from inactivation does not covalently bind to amino acid residues of GABA-AT but stays in the active site via H-bonding interactions with Arg-192, a π−π interaction with Phe-189, and a weak nonbonded S···O═C interaction with Glu-270, thereby inactivating the enzyme.

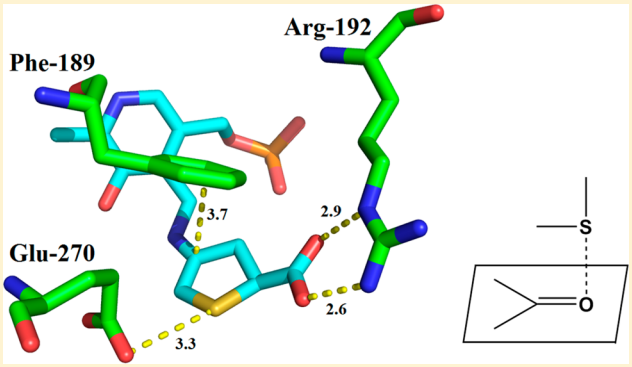

1. INTRODUCTION

Epilepsy is a family of chronic neurological disorders characterized by recurring convulsive seizures, which result from abnormal, excessive neuronal activity in the central nervous system.[1] It is estimated that about 65 million people worldwide have epilepsy.[2] Epilepsy can arise from an imbalance in two major neurotransmitters that regulate brain neuronal activity, L-glutamate, an excitatory neurotransmitter, and γ-aminobutyric acid (GABA), an inhibitory neurotransmitter.[3]

GABA is produced in GABAergic neurons from L-glutamate by the enzyme glutamic acid decarboxylase (GAD) (Figure 1).[4,5] GABA is then released into the synapse and transported to glial cells. The enzyme GABA aminotransferase (GABA-AT) in glial cells degrades GABA to succinic semialdehyde, which is further oxidized to succinate and enters the Krebs cycle. In this first half of the GABA-AT catalytic cycle, the cofactor pyridoxal 5′-phosphate (PLP) is converted to pyridoxamine 5′-phosphate (PMP). GABA-AT also converts α-ketoglutarate from the Krebs cycle to L-glutamate and returns PMP to PLP in the second half of its catalytic cycle. Because there is no GAD in glial cells, this newly formed L-glutamate is not converted to GABA. It is instead converted to L-glutamine, which is then released from glial cells into the synapse and transported back to GABAergic neurons to complete the metabolic cycle of L-glutamate.

Low levels of GABA are linked to not only epilepsy[6] but also many other neurological disorders, including Parkinson's disease,[7] Alzheimer's disease,[8] Huntington's disease,[9] and cocaine addiction.[10] Raising GABA levels has proven effective in stopping recurring convulsive seizures in the treatment of epilepsy.[11] However, GABA does not cross the blood−brain barrier; therefore, an increase in brain levels of GABA cannot be achieved by intravenous administration.[12] To increase brain levels of GABA, one could speed up the activity of GAD, the enzyme that makes GABA; inhibit the activity of GABA-AT, the enzyme that degrades GABA; or inhibit the reuptake of GABA by blocking the action of the GABA transporters.

Received: February 6, 2015
Published: March 17, 2015

DOI: 10.1021/jacs.5b01155
J. Am. Chem. Soc. 2015, 137, 4525−4533

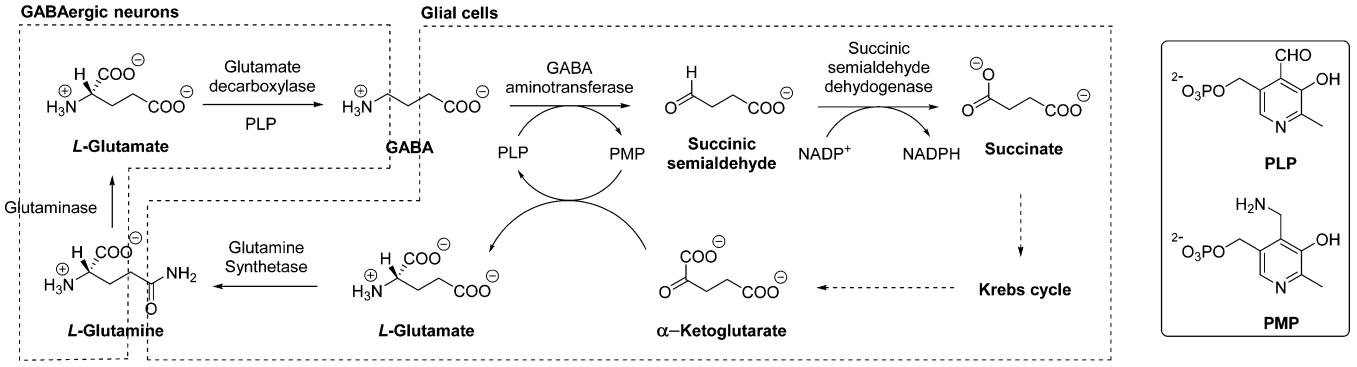

Figure 1. Metabolic cycle of L-glutamate.

Scheme 1. Mechanisms of Inactivation of GABA-AT by Vigabatrin

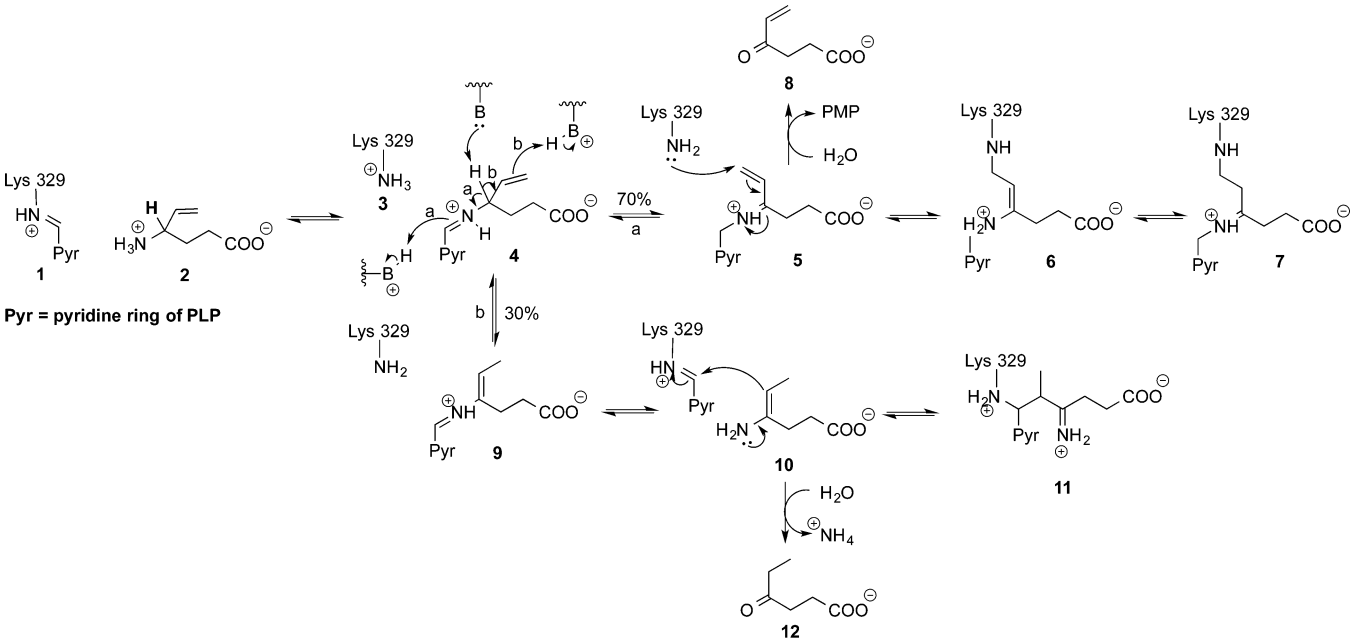

Our laboratory has focused on the design of mechanism-based inactivators of GABA-AT, unreactive compounds that require GABA-AT catalysis to convert them into the species that inactivates the enzyme. Because these molecules are not initially reactive but require the catalytic activity of GABA-AT to become activated and form covalent bonds, indiscriminate reactions with off-target proteins, leading to undesired side effects, should be greatly reduced. Even at lower dosages, these inactivators can achieve the desired pharmacologic effects with enhanced potency and selectivity compared with conventional inhibitors.[13]

Currently, the only U.S. Food and Drug Administration (FDA)-approved inactivator of GABA-AT is the drug vigabatrin (**2**) (Scheme 1), which was first developed by Lippert et al.[14] and is used for the treatment of epilepsy.[15] However, a large dose of vigabatrin (1–3 g) needs to be taken daily,[16−18] and there are many serious side effects that arise from its use, including psychosis[19] and permanent vision loss resulting from damage of the retinal nerve fiber layer.[20] Therefore, the demand for an alternative to vigabatrin in the treatment of epilepsy is urgent.

We have found that vigabatrin inactivates GABA-AT via two pathways: a Michael addition mechanism and an enamine mechanism, as shown in Scheme 1.[21] In the Michael addition mechanism, the Schiff base **4** resulting from the reaction of vigabatrin and the lysine-bound PLP (**1**) on GABA-AT is subjected to removal of the γ-proton (boldfaced hydrogen in **2**) and tautomerization, leading to ketimine **5**. An active-site nucleophile then reacts with Michael acceptor **5** to form **6**, which is in equilibrium with **7**. In the enamine mechanism, Schiff base **4** is subjected to γ-proton removal and tautomerization through the vinyl bond, which leads to the release of enamine **10**. Subsequent nucleophilic addition of **10** to the lysine-bound PLP on GABA-AT gives rise to **11**.

The Michael addition mechanism and the enamine mechanism happen concurrently in a 70/30 ratio, respectively. It was discovered that ketimine **5** in the Michael addition mechanism and enamine **10** in the enamine mechanism undergo partial hydrolysis to form α,β-unsaturated ketone **8** and saturated ketone **12**, respectively. While **8** is a reactive electrophile, possibly responsible for some side effects, **12** is not a reactive metabolite. Therefore, it is imperative to find vigabatrin analogues that either follow the enamine mechanism exclusively to avoid the formation of **8** or speed up the Michael addition pathway so that **5** would have a much lower probability to undergo hydrolysis.

DOI: 10.1021/jacs.5b01155
J. Am. Chem. Soc. 2015, 137, 4525−4533

An energy-minimized molecular model of vigabatrin bound to PLP in GABA-AT revealed that after tautomerization, the vinyl bond in **5** needs to rotate toward Lys-329 for the Michael addition to occur.[22] Conformationally restricted analogues such as **13** and **14** (Figure 2) would prevent the rotation of the vinyl

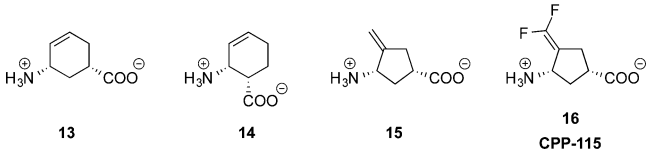

Figure 2. Vigabatrin analogues that follow one GABA-AT inactivation mechanism exclusively.

bond, thereby blocking the Michael addition mechanism. Experiments showed that **13** inactivated GABA-AT following the enamine mechanism exclusively. However, its potency remained low. In the alternative approach, conformationally restricted analogues **15** and **16** have the vinyl bond readily pointed toward Lys-329 for rapid Michael addition to occur, thereby minimizing the hydrolysis of the ketimine intermediate.[23] Experiments showed that **16** was 186 times more efficient in inactivating GABA-AT than vigabatrin. Furthermore, unlike vigabatrin,[24] **16** did not inactivate or inhibit off-target enzymes, such as alanine aminotransferase and aspartate aminotransferase,[25] and therefore is less likely to produce side effects. Indeed, we tested **16** in a multiple-hit rat model of infantile spasms,[26] and the results showed that **16** suppressed spasms at doses of 0.1−1 mg^{-1} kg^{-1} day^{-1}, which were >100-fold lower than those for vigabatrin. The suppression of spasms by **16** stayed effective longer (3 days vs 1 day for vigabatrin), and **16** also had a much larger margin of safety than vigabatrin. With those results, **16**, now known as CPP-115, was granted Orphan Drug Designation by the FDA for the treatment of infantile spasms. It recently finished a phase-I clinical trial.

In our ongoing effort to develop new classes of antiepileptic drugs, we are interested in new GABA analogues that inactivate GABA-AT by new mechanisms. Compounds with a leaving group adjacent to the carbanion formed after the γ-proton removal seem to inactivate GABA-AT by an enamine mechanism. Therefore, we synthesized a series of conformationally restricted tetrahydrothiophene-based analogues (Figure 3) that have a properly positioned leaving group that could

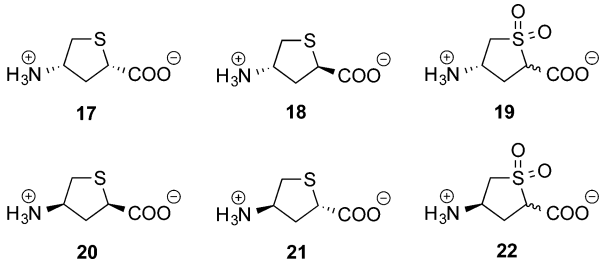

Figure 3. Tetrahydrothiophene-based GABA analogues.

facilitate a ring-opening mechanism in the inactivation of GABA-AT (Scheme 2). Here we report the synthesis, biological evaluation, and mechanistic studies (including mass spectral and X-ray crystallographic results) of these analogues, which reveal an unexpected inactivation mechanism.

Scheme 2. Michael Addition Mechanism (Pathway a) and Enamine Addition Mechanism (Pathway b) for 17

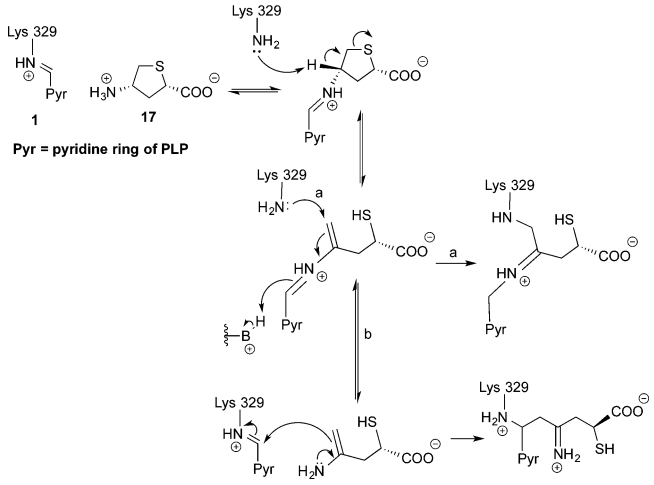

2. RESULTS AND DISCUSSION

The syntheses of analogues **17**−**19** starting from commercially available D-cysteine methyl ester hydrochloride (**23**) are shown in Scheme 3. The route up to the generation of dihydrothiophene **28** was achieved by following a modified version of the procedure of Adams et al.[27] Reduction of **28** by magnesium in methanol resulted in diastereomers **29** and **30**, which were separable by flash column chromatography. Deprotection of the amino group and hydrolysis of the ester in **29** and **30** using aqueous HCl provided the desired analogues **17** and **18**, respectively. Oxidation of **29** or **30** by $MnSO_4$ and H_2O_2 resulted in a 1:1 mixture of the corresponding sulfones **31** as a result of epimerization at C-2. Subsequent deprotection of the amino group and hydrolysis of the ester in **31** using aqueous HCl gave the desired analogue **19**. The syntheses of compounds **20**−**22** followed an identical route starting from L-cysteine methyl ester hydrochloride. The purities of compounds **17**−**22** were confirmed by HPLC and HRMS, which showed that there was none of the corresponding dihydrothiophene analogue of **17**, a known inactivator of GABA-AT.[28]

Preliminary in vitro results showed that **19**−**22** were weak reversible inhibitors, while **17** and **18** were potent inactivators of GABA-AT (Table 1). The kinetic constants for inactivation of GABA-AT by **17** and **18** could not be determined accurately under the optimal conditions (pH 8.5, 25 °C),[23] where the enzyme exhibited maximum activity, because the inactivation occurred too rapidly. The inhibition constants (K_I) and rate constants for enzyme inactivation (k_{inact}) for inactivation of GABA-AT by **17** and **18** were then measured under nonoptimal conditions (pH 6.5, 25 °C) using a Kitz and Wilson replot.[29] From the k_{inact}/K_I values (Table 1), we can conclude that **17** is 8 times more efficient an inactivator of GABA-AT than vigabatrin (with an inhibition constant almost 20 times that of vigabatrin) and that **18** is half as efficient as vigabatrin.

The X-ray crystal structure GABA-AT inactivated by **17** (at 1.66 Å) showed that the inactivating metabolite contained a buckled five-membered ring covalently bound to PLP (Figure 4A) and that Lys-329 was not covalently modified. The final ligand interpretation is strongly supported by the electron density of the simulated-annealing omit map ($F_o - F_c$). Furthermore, the omit map density at a higher contour level

DOI: 10.1021/jacs.5b01155
J. Am. Chem. Soc. 2015, 137, 4525−4533

Scheme 3. Syntheses of GABA Analogues 17−19

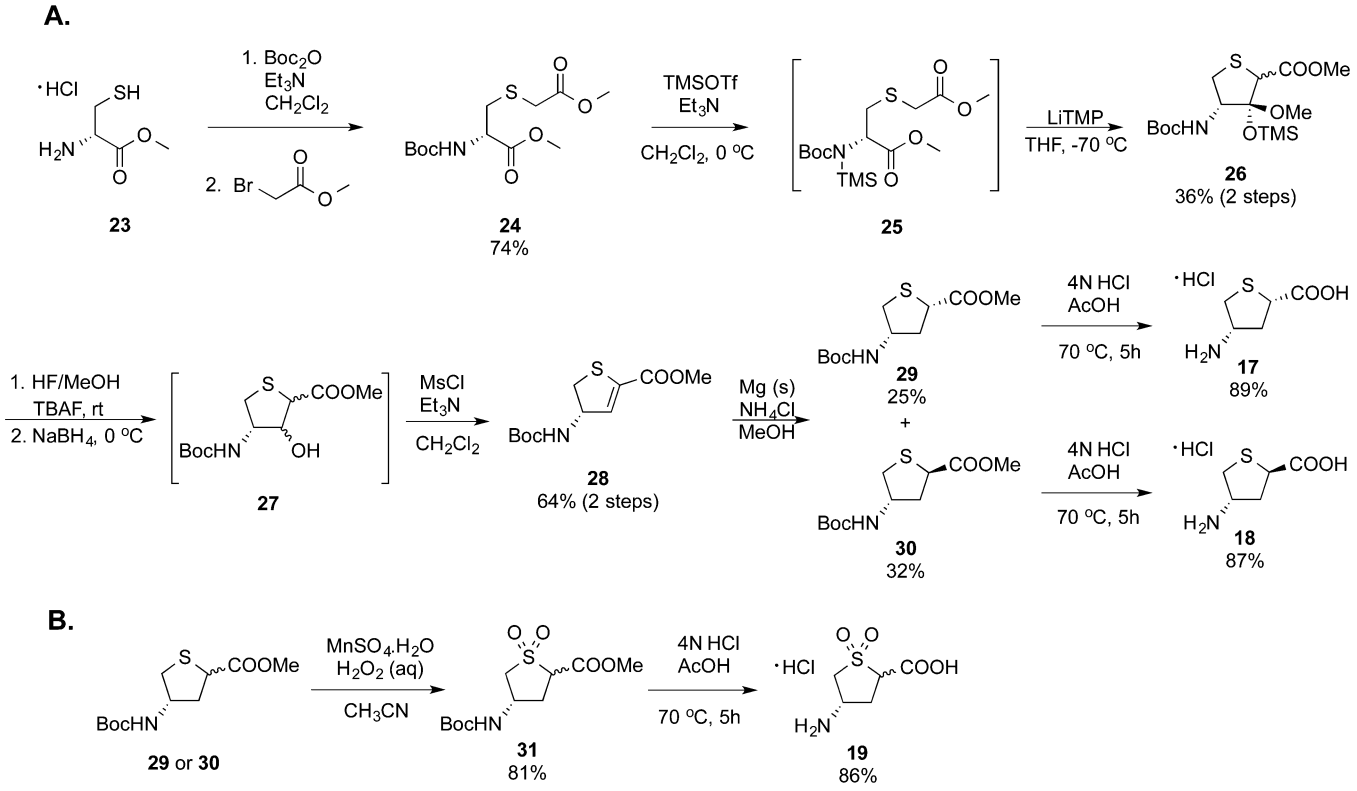

Table 1. Kinetic Constants for the Inhibition and Inactivation of GABA-AT by 17−19

compound	K_I (mM)	k_{inact} (min^{-1})	k_{inact}/K_I (min^{-1} mM^{-1})	K_i (mM)
17	0.182	0.17	0.93	–
18	2.23	0.12	0.05	–
19	–	–	–	3.2 ± 0.7
20	–	–	–	3.4 ± 0.8
21	–	–	–	3.3 ± 0.7
22	–	–	–	7.5 ± 0.7
(*S*)-vigabatrin	3.2	0.37	0.11	–

also revealed that the refined atom positions of the dihydrothiophene ring were accurate, resulting in a nonplanar ring (Figure 4B,C). (*S*)-4-Amino-4,5-dihydro-2-thiophenecarboxylic acid, the corresponding dihydrothiophene analogue of **17**, is a known inactivator of GABA-AT that inactivates by an aromatization mechanism resulting in a thiophene ring;[28] it also is an inactivator of aspartate aminotransferase.[30] Here the crystal structure of **17**-inactivated GABA-AT suggests that the inactivation by **17** is likely to follow the mechanism shown in Scheme 4. The Schiff base **32** resulting from the reaction of **17** and the lysine-bound PLP on GABA-AT undergoes γ-proton removal, leading to enamine **34**. The crystal structure revealed that **34** is stabilized in the active site by an interaction between its carboxylate group and the guanidinum group of Arg-192 and an interaction between the enamine alkene and the phenyl ring of Phe-189 (Figure 5A). Also, the sulfur atom in **34** is in close proximity (3.3 Å) to a carboxyl oxygen atom of Glu-270. This distance suggests a weak nonbonded interaction between the divalent sulfur and the carboxyl carbonyl oxygen. Weak nonbonded S···O and S···N interactions have been reported and are mainly characterized as stabilizing forces of protein structures[31] and of some organic sulfur compounds.[32,33] These interactions have recently attracted growing attention because they could play important roles in the structure and biological activity of some sulfur compounds and might also regulate enzymatic functions.[34] To date, all reported weak nonbonded interactions have been intramolecular. To the best of our knowledge, no intermolecular weak nonbonded S···O and S···N interactions have been reported. However, the distance and directionality of intermolecular nonbonded S···O interactions have been suggested in theoretical studies.[34] For intermolecular nonbonded S···O interactions, the nucleophilic O atom approaches the S atom from the back side of the S−Y and S−Z bonds (the σ_s^* direction), and the S atom lies in the direction of the O lone pairs (the n_O direction) (Figure 5B). The stabilization of this S···O=C interaction is described by an $n_O \rightarrow \sigma_s^*$ orbital interaction, and 3.3 Å is well within the predicted distance. As shown in Figure 5A, the directionality of the interaction between the sulfur atom in metabolite **34** and the carboxyl group of Glu-270 matches the description of the directionality of theoretical intermolecular nonbonded S···O interactions. Therefore, the interaction between the sulfur atom in metabolite **34** and the carboxyl group of Glu-270 might be the first reported example of an intermolecular nonbonded S···O interaction, which contributes to the stabilization of metabolite **34** in the active site of GABA-AT.

Mass spectrometric analysis (via electrospray ionization mass spectrometry) was run on a sample of GABA-AT inactivated by **17**, but the presence of **34** was not observed. When a small amount of formic acid was added to another sample of GABA-AT inactivated by **17** to disrupt the H-bonding before the spectrum was run, metabolite **36** (*m*/*z* 144.9954; Figure S1 in the Supporting Information) was detected instead of **34**. Fragmentation data for *m*/*z* 144.9954 (Figure S2 in the

DOI: 10.1021/jacs.5b01155
J. Am. Chem. Soc. 2015, 137, 4525−4533

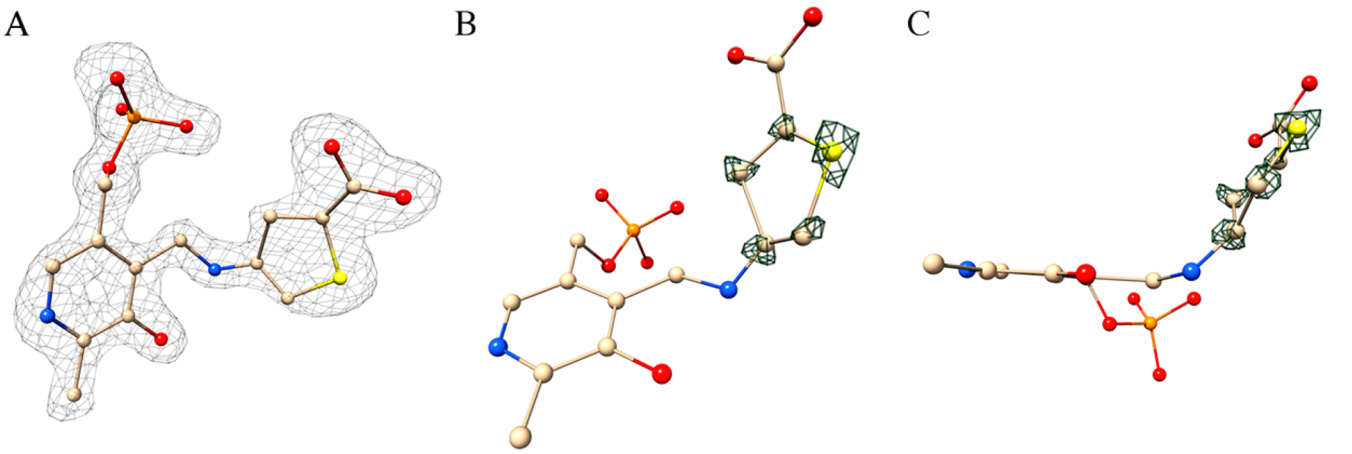

Figure 4. The PLP−dihydrothiophene complex, shown in ball-and-stick form, is the final adduct, which contains a nonplanar dihydrothiophene ring. Carbons are in beige, nitrogens are in blue, oxygens are in red, phosphorus is in orange, and sulfur is in yellow. (A) The electron density of the simulated-annealing omit map ($F_o - F_c$) is shown as a gray mesh at 3.5σ around the PLP−dihydrothiophone adduct. (B, C) Two different orientations of the same image, displaying (B) the refined atom positions and (C) the buckled ring plane. The electron density of the simulated omit map ($F_o - F_c$) is shown in green mesh at 4.1σ around atoms in the dihydrothiophene ring (at a radius of 0.6 Å).

Scheme 4. Proposed Mechanism for the Inactivation of GABA-AT by 17

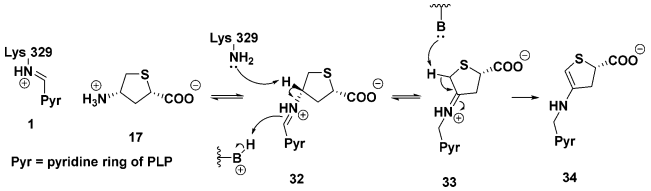

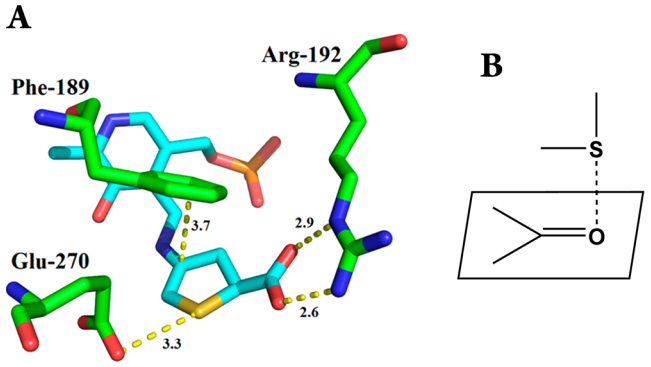

Figure 5. (A) Interactions between the PLP−dihydrothiophene adduct and nearby residues. (B) Directionality of the intermolecular weak nonbonded S···O interaction in theoretical studies,[34] representing an $n_O \rightarrow \sigma^*_s$ orbital interaction.

Supporting Information) confirmed the structure of **36**, the likely result of hydrolysis of **34** (Scheme 5).

Treatment of [7-^{3}H]PLP-reconstituted GABA-AT with **17** was performed to determine the fate of the coenzyme upon inactivation. A solution of 1 mM PMP and 1 mM PLP was treated identically as a control. The results showed that the denaturation of GABA-AT inactivated by **17** released PMP exclusively (Figure 6).

The results of the radioactive-labeling experiment and mass spectrometric analysis suggested that metabolite **34** is not stable outside of the active site and undergoes hydrolysis to produce PMP and **36**, supporting the proposed mechanism for the inactivation of GABA-AT by **17** shown in Scheme 4.

Scheme 5. Hydrolysis of Metabolite 34

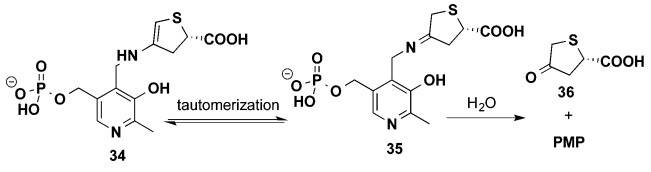

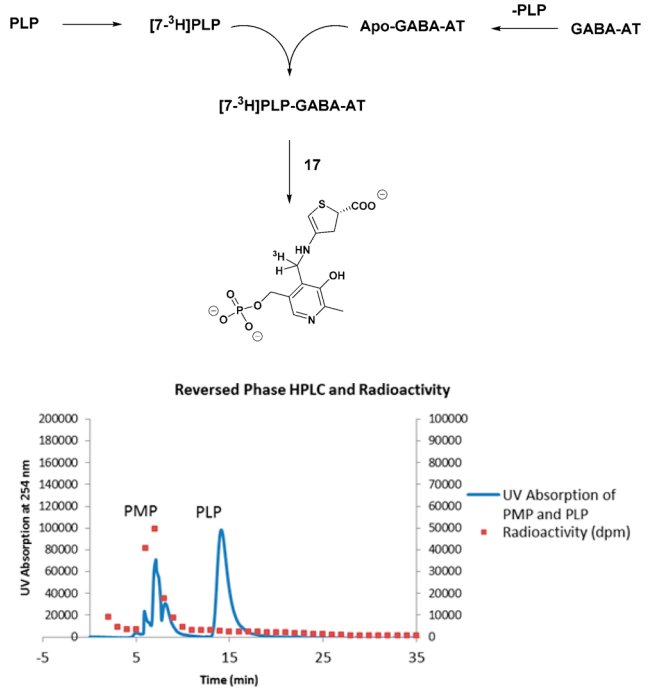

Figure 6. Radioactive-labeling experiment for the inactivation of GABA-AT by **17**: [7-^{3}H]PLP−GABA-AT was prepared from apo-GABA-AT and [7-^{3}H]PLP and then inactivated by **17**, followed by denaturation and submission to HPLC. Fractions were collected each minute and counted for radioactivity. A solution of 1 mM PMP and 1 mM PLP was treated identically as a control.

DOI: 10.1021/jacs.5b01155
J. Am. Chem. Soc. 2015, 137, 4525−4533

If the interaction between the sulfur atom in **34** and the O=C of Glu-270 is an intermolecular nonbonded S···O interaction, then the corresponding cyclopentane analogue **39** (Scheme 6)

Scheme 6. Synthesis of Cyclopentane Analogue 39

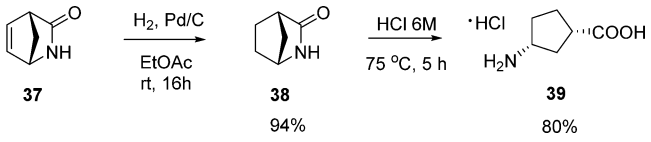

should form a less stable metabolite in the active site of GABA-AT than **34**. We synthesized **39** from (1*S*,4*R*)-2-azabicyclo-[2.2.1]hept-5-en-3-one (**37**) (Scheme 6) and investigated its activity. The results showed that **39** is not an inactivator but is a good competitive inhibitor of GABA-AT with K_i = 0.87 mM. A computer model of the energy-minimized hypothetical adduct of **39** bound to PLP after tautomerization and deprotonation (i.e., the cyclopentene analogue of **34**) docked into GABA-AT using GOLD[35] gave the pose with the highest fitness score that was almost identical to that shown in Figure 5 (Figure S25 in the Supporting Information). These inhibition and modeling results further support the crucial role of the sulfur atom in retaining the product in the active site of GABA-AT, thereby inactivating the enzyme.

3. CONCLUSION

We have developed two new GABA-AT inactivators. Preliminary in vitro results showed that **17** is 8 times more efficient an inactivator of GABA-AT than vigabatrin, an FDA-approved antiepilepsy drug, and that **18** is half as efficient as vigabatrin. Mechanistic studies of the inactivation of GABA-AT by **17** showed that the sulfur atom in **17** plays a crucial role in keeping the resulting adduct bound to the active site of GABA-AT, thereby inactivating the enzyme. An intermolecular nonbonded interaction between the carboxyl oxygen of Glu-270 and the sulfur atom in **17**, the first observed example of this kind, is important for stabilizing the adduct in the active site.

4. EXPERIMENTAL SECTION

General Procedures. Chemicals were obtained from TCI America, Sigma-Aldrich, Alfa Aesar, and American Radiolabeled Chemicals and used as received, unless otherwise specified. All of the syntheses were conducted under anhydrous conditions in an atmosphere of argon using flame-dried apparatus and employing standard techniques to handle air-sensitive materials, unless otherwise noted. All of the solvents were distilled and stored under an argon or nitrogen atmosphere before use. ^{1}H and ^{13}C NMR spectra were taken on a Bruker AVANCE III 500 spectrometer using $CDCl_3$, MeOD, $(CD_3)_2CO$, or D_2O as the solvent. Chemical shifts (δ) were recorded in parts per million and referenced to $CDCl_3$ (7.26 ppm for ^{1}H NMR and 77.16 ppm for ^{13}C NMR), MeOD (3.31 ppm for ^{1}H NMR and 49.00 ppm for ^{13}C NMR), $(CD_3)_2CO$ (2.05 ppm for ^{1}H NMR and 29.84 ppm for ^{13}C NMR), or D_2O (4.79 ppm for ^{1}H NMR). Nuclear Overhauser effect (NOE) correlation experiments were performed using an Agilent DDR2 400 MHz spectrometer. High-resolution mass spectrometry (HRMS) was performed with an Agilent 6210 LC-TOF (ESI, APCI, APPI) mass spectrometer. The purities of the synthesized final compounds were determined by HPLC analysis to be >95%. A Chiralcel OD-H 5 μm, 4.6 mm × 250 mm column was used. After thorough column equilibration, compounds were eluted with a mobile phase of 2% EtOH in hexanes at 0.6 mL/min. Biochemical assays were performed using a Biotek Synergy H1 microplate reader. Prior to their evaluation, initial experiments were performed to confirm that the synthesized analogues did not inhibit the coupling enzymes utilized in the substrate and inhibition assays. For mass spectrometric analysis, the LC gradient was employed at a flow rate of 200 μL/min on an Agilent 1150 LC system (Agilent, Santa Clara, CA, USA), and mass spectrometry was performed on a Q-Exactive mass spectrometer (Thermo Fisher Scientific, Waltham, MA, USA). Crystallographic data were collected on beamlines 23ID-B and 23ID-D of GM/CA@APS of the Advanced Photon Source (APS) using X-rays with a wavelength of 0.99 Å and a Rayonix (formerly MAR-USA) 4 × 4 tiled CCD detector with a 300 mm^2 sensitive area.

(*S*)-Methyl 2-((*tert*-Butoxycarbonyl)amino)-3-((2-methoxy-2-oxoethyl)thio)propanoate (24). To a stirred light suspension of D-cysteine methyl ester hydrochloride (**23**) (5 g, 29.1 mmol) and Boc_2O (7 mL, 30.6 mmol) in anhydrous CH_2Cl_2 (250 mL) at 0 °C was added Et_3N (15.4 mL, 111 mmol) over a 10 min period. After addition, the cooling bath was removed, and the reaction solution was stirred at room temperature (rt) overnight. After the reaction solution was cooled to 0 °C, methyl bromoacetate (3.3 mL, 35 mmol) was added, and the resulting mixture was stirred for 30 min before removal of the cooling bath. Stirring was continued for 2 h at rt, followed by removal of the bulk of the solvent under reduced pressure. The resulting crude mixture was diluted with ether (60 mL), washed with water (3 × 30 mL) and brine (5 mL), dried ($MgSO_4$), and concentrated. Chromatography (ethyl acetate/hexanes, 3:7) afforded the desired product as a clear oil (6.79 g, 74%). The ^{1}H NMR data matched the literature values.[27] ^{1}H NMR (500 MHz, $CDCl_3$) δ 5.40 (d, J = 8.2 Hz, 1H), 4.55 (m, 1H), 3.75 (s, 3H), 3.73 (s, 3H), 3.26 (q, J = 15.2 Hz, 2H), 3.07 (m, 2H), 1.43 (s, 9H). ^{13}C NMR (126 MHz, $CDCl_3$) δ 171.50, 170.61, 155.27, 80.35, 53.16, 52.78, 52.66, 35.02, 33.90, 28.38. HRMS (LC-TOF): calcd for $C_{12}H_{21}NO_6S$ $[M + Na]^+$ 330.0982; found 330.1001.

(3*R*,4*S*)-Methyl 4-((*tert*-Butoxycarbonyl)amino)-3-methoxy-3- ((trimethylsilyl)oxy)tetrahydrothiophene-2-carboxylate (26). To a solution of **24** (6.59 g, 21.4 mmol) in anhydrous dichloromethane (100 mL) at 0 °C was added Et_3N (3.3 mL, 23.6 mmol), followed by dropwise addition of TMSOTf (4.25 mL, 23.5 mmol) over 20 min. The mixture was stirred for 10 min at 0 °C and then allowed to warm to rt. After the reaction was quenched with saturated sodium bicarbonate (50 mL), the organic layer was separated, washed with saturated $NaHCO_3$ (2 × 50 mL), dried ($MgSO_4$), and concentrated to obtain crude intermediate **25**.

In a separate flask, a solution of lithium tetramethylpiperidide was prepared by dropwise addition of *n*-BuLi (14.0 mL, 22.4 mmol; 1.6 M solution in hexanes) to a solution of 2,2,6,6-tetramethylpiperidine (4.17 mL, 24.5 mmol) in THF (100 mL) at −78 °C. After a brief warmup to rt, the solution was cooled to −78 °C, and crude intermediate **25** in THF (50 mL) was added dropwise over 30 min. After the addition, the reaction mixture was stirred at −78 °C for 30 min and at −40 °C for another 30 min. The reaction mixture was cooled again to −78 °C, and the reaction was quenched with acetic acid (3 mL). The reaction mixture was diluted in ether (100 mL), washed with water (3 × 100 mL), 0.5 N HCl (3 × 30 mL), and brine (10 mL), dried ($MgSO_4$), and concentrated. The crude product was purified by chromatography (ethyl acetate/hexanes, 3:17) to yield the major diastereomer **26** as a white solid (2.91 g, 36%). The ^{1}H NMR data matched the literature values.[27] ^{1}H NMR (500 MHz, $CDCl_3$) δ 6.76 (d, J = 9.5 Hz, 1H), 4.22 (ddd, J = 9.6, 5.1, 1.8 Hz, 1H), 4.06 (s, 1H), 3.70 (s, 3H), 3.31 (s, 3H), 3.23 (dd, J = 10.9, 5.1 Hz, 1H), 2.80 (dd, J = 10.9, 1.9 Hz, 1H), 1.40 (s, 9H), 0.11 (s, 9H). ^{13}C NMR (126 MHz, $CDCl_3$) δ 173.09, 155.37, 110.31, 79.39, 59.44, 52.83, 50.78, 49.65, 36.83, 28.50, 0.89. HRMS (LC-TOF): calcd for $C_{15}H_{29}NO_6SSi$ $[M + Na]^+$ 402.1377; found 402.1388.

(*S*)-Methyl 4-((*tert*-Butoxycarbonyl)amino)-4,5-dihydrothiophene-2-carboxylate (28). To a stirred solution of **26** (979 mg, 2.58 mmol) in 1 M HF solution (13 mL, prepared by dilution of 48% aqueous HF in dry methanol) at rt was added TBAF (2.84 mL, 2.84 mmol; 1 M solution in THF). The reaction mixture was stirred at rt for 2 h and then cooled in an ice/brine bath, after which $NaBH_4$ (199 mg, 5.16 mmol) was added in small portions while the reaction temperature was maintained at 0 °C. Following addition, the reaction mixture was stirred for 1 h at 0 °C, and then the reaction was

DOI: 10.1021/jacs.5b01155
J. Am. Chem. Soc. 2015, 137, 4525−4533

quenched with acetone (1.3 mL) and the mixture was allowed to continue stirring at rt. After 1 h, acetic acid (161 μL) was added, followed by removal of most of the solvent under reduced pressure. The resulting crude mixture was diluted with ethyl acetate (30 mL), washed with 1:1 saturated brine/water (15 mL), water (2 × 15 mL), and brine (3 mL), dried ($MgSO_4$), and concentrated to yield the crude alcohol, which was used in the next step without purification.

To a stirred solution of the crude alcohol in CH_2Cl_2 (13 mL) at 0 °C was added Et_3N (1.44 mL, 10.3 mmol) followed by mesyl chloride (400 μL, 5.17 mmol) dropwise. The reaction mixture was stirred for 30 min at 0 °C and overnight at rt. After removal of most of the solvent under reduced pressure, the resulting crude mixture was diluted with ethyl ether (30 mL), washed with water (2 × 15 mL), 0.5 M HCl (15 mL), and brine (3 mL), dried ($MgSO_4$), and concentrated. Chromatography (ethyl acetate/hexanes, 3:7) afforded the desired product as a white solid (430 mg, 64%). ^{1}H NMR (500 MHz, $CDCl_3$) δ 6.51 (d, J = 3.3 Hz, 1H), 5.15 (m, 1H), 4.90 (d, J = 9.2 Hz, 1H), 3.79 (s, 3H), 3.61 (dd, J = 12.3, 8.3 Hz, 1H), 3.13 (dd, J = 12.3, 4.2 Hz, 1H), 1.43 (s, 9H). ^{13}C NMR (126 MHz, $CDCl_3$) δ 162.68, 154.74, 138.37, 131.93, 80.35, 58.29, 52.76, 39.40, 28.44. HRMS (LC-TOF): calcd for $C_{11}H_{17}NO_4S$ $[M + Na]^+$ 282.0770; found 282.0773.

(2*S*,4*S*)- and (2*R*,4*S*)-Methyl 4-((*tert*-Butoxycarbonyl)amino)-tetrahydrothiophene-2-carboxylate (29 and 30). Magnesium turnings (484 mg, 19.9 mmol) were added to a mixture of (*S*)-methyl 4-((*tert*-butoxycarbonyl)amino)-4,5-dihydrothiophene-2-carboxylate (**28**) (430 mg, 1.66 mmol) and NH_4Cl (5.33 g, 99.6 mmol) in MeOH (15 mL), and the resulting mixture was vigorously stirred overnight at rt. After removal of most of the solvent under reduced pressure, the resulting crude mixture was diluted with water (20 mL) and extracted with ethyl ether (3 × 40 mL). The combined organic layers were washed with brine (2 mL), dried ($MgSO_4$), and concentrated. Chromatography (ethyl ether/toluene, 2:8) afforded **29** (109 mg, 25%) and **30** (141 mg, 32%) as white solids. Data for **29**: ^{1}H NMR (500 MHz, $CDCl_3$) δ 5.86 (d, J = 7.6 Hz, 1H), 4.55−4.40 (m, 1H), 3.97 (dd, J = 8.6, 3.1 Hz, 1H), 3.72 (s, 3H), 3.11 (dd, J = 11.0, 5.0 Hz, 1H), 2.92 (dd, J = 11.3, 3.6 Hz, 1H), 2.37−2.26 (m, 1H), 2.17 (ddd, J = 14.0, 8.5, 6.0 Hz, 1H), 1.41 (s, 9H). ^{13}C NMR (126 MHz, $CDCl_3$) δ 175.10, 155.31, 79.48, 55.54, 52.95, 45.68, 40.16, 37.28, 28.48. HRMS (LC-TOF): calcd for $C_{11}H_{19}NO_4S$ $[M + Na]^+$ 284.0927; found 284.0931. Data for **30**: ^{1}H NMR (500 MHz, $(CD_3)_2CO$) δ 6.25 (d, J = 3.4 Hz, 1H), 4.49 (tt, J = 7.4, 3.8 Hz, 1H), 4.06 (dd, J = 7.5, 5.1 Hz, 1H), 3.69 (s, 3H), 3.14 (dd, J = 10.5, 5.6 Hz, 1H), 2.78 (dd, J = 10.5, 6.2 Hz, 1H), 2.42 (dt, J = 13.0, 5.3 Hz, 1H), 2.15−2.05 (m, 1H), 1.42 (s, 9H). ^{13}C NMR (126 MHz, $(CD_3)_2CO$) δ 174.00, 155.92, 78.96, 55.98, 52.52, 44.49, 37.69, 37.53, 28.53. HRMS (LC-TOF): calcd for $C_{11}H_{19}NO_4S$ $[M + Na]^+$ 284.0927; found 284.0931.

(2*S*,4*S*)-4-Aminotetrahydrothiophene-2-carboxylic Acid Hydrochloride (17). Boc-protected amino acid ester **29** (100 mg, 0.38 mmol) was dissolved in 4 N HCl (5 mL) and acetic acid (5 mL). The resulting solution was heated to 70 °C and stirred for 5 h before being concentrated in vacuo to afford a solid. The solid was purified by ion-exchange chromatography (AG 50W-X8), eluting with a gradient from 0.4 to 2.0 N HCl, giving the desired amino acid hydrochloride product as a white solid (63 mg, 89%). ^{1}H NMR (500 MHz, MeOD) δ 4.10 (m, 2H), 3.32 (dd, J = 11.8, 5.6 Hz, 1H), 3.09 (dd, J = 11.8, 5.0 Hz, 1H), 2.52−2.43 (m, 1H). ^{13}C NMR (126 MHz, MeOD) δ 177.11, 55.99, 46.14, 37.28, 36.77. HRMS (LC-TOF): calcd for $C_5H_9NO_2S$ $[M - H]^-$ 146.0281; found 146.0278.

(2*R*,4*S*)-4-Aminotetrahydrothiophene-2-carboxylic Acid Hydrochloride (18). Compound **18** (61 mg, 87%) was synthesized from **30** (100 mg, 0.38 mmol) by a procedure similar to that used to obtain **17** from **29**. ^{1}H NMR (500 MHz, MeOD) δ 4.15 (p, J = 5.9 Hz, 1H), 4.05 (dd, J = 7.6, 4.5 Hz, 1H), 3.28 (dd, J = 11.6, 5.7 Hz, 1H), 2.95 (dd, J = 11.5, 5.7 Hz, 1H), 2.65 (dt, J = 13.6, 5.0 Hz, 1H), 2.18 (dt, J = 13.9, 7.2 Hz, 1H). ^{13}C NMR (126 MHz, MeOD) δ 175.62, 55.75, 45.19, 37.22, 35.81. HRMS (LC-TOF): calcd for $C_5H_9NO_2S$ $[M - H]^-$ 146.0281; found 146.0278.

(4*S*)-Methyl 4-((*tert*-Butoxycarbonyl)amino)tetrahydrothiophene-2-carboxylate 1,1-Dioxide (31). To a stirred solution of **29** (60 mg, 0.23 mmol) and $MnSO_4 \cdot H_2O$ (1 mg) in CH_3CN (5 mL) was added at room temperature a mixture of 30% H_2O_2 (1.15 mmol, 118 μL) and 0.2 M $NaHCO_3$ (3.4 mL), previously prepared at 0 °C. After 15 min the reaction was quenched with brine, and the resulting mixture was extracted with ethyl acetate (3 × 10 mL), dried (Na_2SO_4), and concentrated. Chromatography (ethyl acetate/hexanes; 1:9) provided the desired product as a 1:1 mixture of two diastereomers (55 mg, 81%). ^{1}H NMR (500 MHz, $CDCl_3$) δ [5.57 (d, J = 7.1 Hz); 5.21 (d, J = 6.2 Hz), 1H], [4.65 (br s), 4.54 (sex, J = 6.6 Hz), 1H], [4.14 (t, J = 7.9 Hz), 4.11 (dd, J = 9.1, 6.1 Hz), 1H], [3.88 (s), 3.85 (s), 3H], [3.47 (dd, J = 13.5, 6.9 Hz), 3.42 (dd, J = 13.7, 7.0 Hz), 1H], [3.18 (t, J = 4.9 Hz), 3.15 (t, J = 5.4 Hz), 1H], [2.83 (dt, J = 13.9, 6.8 Hz), 2.69 (ddd, J = 14.1, 8.9, 6.9 Hz), 1H], 2.50 (m, 1H), 1.44 (s, 9H). ^{13}C NMR (126 MHz, $CDCl_3$) δ [166.49, 165.77], [155.00, 154.78], [80.76, 80.59], [65.14, 64.02], [57.07, 56.05], [53.98, 53.78], [45.54, 45.37], [33.30, 32.23], [28.43, 28.41]. HRMS (LC-TOF): calcd for $C_{11}H_{19}NO_6S$ $[M + Na]^+$ 316.0825; found 316.0833.

(4*S*)-4-Aminotetrahydrothiophene-2-carboxylic Acid 1,1-Dioxide Hydrochloride (19). Compound **19** was synthesized from **31** as an inseparable 1:1 mixture of diastereomers by a procedure similar to that used to obtain **17** from **29** (86%). ^{1}H NMR (500 MHz, MeOD) δ [4.41 (dd, J = 8.6, 4.9 Hz), 4.36 (dd, J = 9.5, 7.9 Hz), 1H], [4.27 (p, J = 7.4 Hz), 4.12 (p, J = 8.1 Hz), 1H], [3.73 (dd, J = 13.8, 8.1 Hz), 3.68 (dd, J = 13.8, 8.0 Hz), 1H], [3.35 (dd, J = 13.9, 7.1 Hz), 3.29 (dd, J = 13.5, 8.1 Hz), 1H], [2.96 (ddd, J = 14.2, 7.0, 5.0 Hz), 2.84 (dt, J = 14.2, 7.2 Hz), 1H], [2.55 (dt, J = 13.9, 9.3 Hz), 2.46 (dt, J = 14.3, 8.1 Hz), 1H]. ^{13}C NMR (126 MHz, MeOD) δ [167.13, 167.04], [66.52, 65.56], [54.61, 54.44], [46.38, 45.40], [31.40, 31.37]. HRMS (LC-TOF): calcd for $C_5H_9NO_4S$ $[M + Na]^+$ 202.0144; found 202.014.

(1*R*,4*S*)-2-Azabicyclo[2.2.1]heptan-3-one (38). Compound **38** was prepared from (1*S*,4*R*)-2-azabicyclo[2.2.1]hept-5-en-3-one (**37**) by following a published procedure (94%).[36] The ^{1}H NMR data matched the literature values.[37] ^{1}H NMR (500 MHz, $CDCl_3$) δ 5.53 (br s, 1H), 3.90 (m, 1H), 2.76 (m, 1H), 1.95−1.40 (m, 6H). ^{13}C NMR (126 MHz, $CDCl_3$) δ 181.05, 55.54, 45.04, 41.37, 30.34, 23.79. HRMS (LC-TOF): calcd for C_6H_9NO $[M + Na]^+$ 134.0576; found 134.0578.

Preparation of (1*S*,3*R*)-3-Aminocyclopentane-1-carboxylic Acid Hydrochloride (39). Compound **39** was prepared from **38** by following a published procedure (80%).[37] The ^{1}H NMR data matched the literature values.[37] ^{1}H NMR (500 MHz, D_2O) δ 3.76 (m, 1H), 3.01 (m, 1H), 2.44−1.79 (m, 6H). ^{13}C NMR (126 MHz, D_2O) δ 180.01, 51.47, 42.40, 33.65, 29.81, 27.68. HRMS (LC-TOF): calcd for $C_6H_{11}NO_2$ $[M + H]^+$ 130.0863; found 130.0864.

Purification of GABA Aminotransferase (GABA-AT) from Pig Brain. GABA-AT was isolated and purified from pig brain by a published procedure.[38] The purified GABA-AT used in these experiments was found to have a concentration of 6.41 mg/mL with a specific activity of 1.84 units/mg.

Evaluation of Compounds as Time-Dependent Inhibitors of GABA-AT. GABA-AT (17.5 μL) was incubated in the presence of various concentrations of each compound (70 μL final volume) at 25 °C in 50 mM potassium pyrophosphate buffer solution (pH 6.5) containing 5 mM α-ketoglutarate and 1 mM β-mercaptoethanol. Aliquots (10 μL) were withdrawn at timed intervals and were added immediately to the assay solution (137 μL, see below) followed by the addition of the enzyme succinic semialdehyde dehydrogenase (SSDH) (3 μL). The relative enzyme activity was determined by normalizing the rate of increasing absorbance at 340 nm to a control. A Kitz and Wilson replot was used to determine the kinetic constants K_I and k_{inact}.[29]

Evaluation of Compounds as Inhibitors of GABA-AT. Inhibition constants were determined by monitoring the GABA-AT activity in the presence of 0−50 mM concentrations of the synthesized analogues using a coupled assay with SSDH. The assay solution consisted of 10 mM GABA, 5 mM α-ketoglutarate, 1 mM $NADP^+$, 5 mM β-mercaptoethanol, and excess SSDH in 50 mM potassium pyrophosphate buffer (pH 8.5). The enzyme activity was determined by observing the change in absorbance at 340 nm at 25 °C. Half-maximal inhibitory concentration (IC_{50}) values were obtained using nonlinear regression in GraphPad Prism5 software. Subsequent K_i values were determined using the Cheng−Prusoff relationship.[39]

DOI: 10.1021/jacs.5b01155
J. Am. Chem. Soc. 2015, 137, 4525−4533

Evaluation of Compounds as Substrates for GABA-AT. Compounds were tested using an experiment in which the conversion of α-ketoglutarate to L-glutamic acid was monitored as an indication of the rate of PLP reduction to PMP, which in turn corresponds to amine oxidation to the corresponding aldehyde. Enzyme reactions were prepared at 5 mM concentrations of compounds in 100 μL of pyrophosphate buffer (50 mM, pH 8.5) containing 5 mM α-ketoglutarate and 0.13 mg/mL purified GABA-AT and allowed to incubate at room temperature for 24 h. The L-glutamic acid content was determined by combining 50 μL of each incubation mixture with 50 μL of Tris-HCl buffer (100 mM, pH 7.5) containing 100 μM Ampliflu Red (Sigma-Aldrich), 0.25 units/mL horseradish peroxidase, and 0.08 units/mL L-glutamate oxidase in a 96-well black-walled plate. After incubation at 37 °C for 30 min, the fluorescence was recorded with the aid of a microplate reader (BioTek Synergy H1) at an excitation wavelength of 530 nm and an emission wavelength of 590 nm; the fluorescence was proportional to the L-glutamate concentration.

Preparation of [7-^{3}H]Pyridoxal 5′-Phosphate ([7-^{3}H]PLP). To a solution of pyridoxal 5′-phosphate (PLP) in water (1.8 mL, 0.28 M) was added 30 drops of 1 M NaOH. The mixture was then cooled to 0 °C in an ice bath, and a solution of $NaBH_4$ (5.86 mg, 0.15 mmol) and $NaB[^3H]_4$ (100 mCi) in 450 μL of 0.1 M NaOH was added in small portions; the resulting mixture was stirred for 1 h at 0 °C. Concentrated HCl (120 μL) was then added to the solution very slowly (the pH of the resulting solution was 4), and the reaction mixture was stirred for 5 min at 0 °C. Ground MnO_2 (200 mg, 2.3 mmol) was added, and the resulting mixture was stirred for 2 h at rt. A solution of 1 M NaOH was added dropwise to bring the pH to 8, and the resulting solution was centrifuged. The supernatants were collected and loaded onto a gel filtration column packed with Bio-Rad AG1-X8 resin (hydroxide form). Water/5 M acetic acid was used as the mobile phase (gradient from 90% water to 0% water, 1.5 mL/min, 300 min). Fractions (10 mL each) were collected and tested for UV absorption and radioactivity. The fractions with the desired product were lyophilized and then loaded onto an HPLC with a Phenomenex Gemini C18 column (4.6 mm × 250 mm, 5 μm, 110 A). Water (with 0.1% TFA)/acetonitrile (with 0.1% TFA) was used as the mobile phase (5% acetonitrile, 0.5 mL/min, 25 min; then gradient to 95% acetonitrile, 0.5 mL/min, 20 min). Under these conditions, PLP eluted at 38 min. Fractions running with the PLP peak were collected, counted for radioactivity using liquid scintillation counting, and then lyophilized, affording [7-^{3}H]PLP.

Preparation of [7-^{3}H]PLP-Reconstituted GABA-AT. To potassium phosphate buffer (0.5 mL, 100 mM, pH 7.4) containing β-mercaptoethanol (0.25 mM) (buffer A) and GABA-AT (170 μg, 1.55 nmol) protected from light was added GABA (10 mg, 0.097 mmol). The resulting solution was stirred at rt for 1 h and then dialyzed at 4 °C against potassium phosphate buffer (200 mL, 500 mM, pH 5.5) containing β-mercaptoethanol (0.25 mM) (buffer B) and GABA (4.0 g, 39 mmol) for 3 h. The solution was then dialyzed at 4 °C against 1800 mL of buffer B overnight, followed by dialysis at 4 °C against 4 × 500 mL of potassium phosphate buffer (100 mM, pH 8.0) containing β-mercaptoethanol (0.25 mM) (buffer C) at 1.5 h intervals. An aliquot (1 μL) of the dialyzed solution was assayed to confirm that no enzyme activity remained. To the dialyzed solution of enzyme (apo-GABA-AT) was added a solution of PLP (40 μL, 20 mM) and [^{3}H]PLP (one-fifth of the amount prepared above), and the mixture was stirred at rt for 5 h until the enzyme activity returned and the reactivation was complete. The excess [^{3}H]PLP was removed from the reconstituted GABA-AT solution by centrifugation with 5 × 400 μL of buffer C using a 10k molecular weight cutoff filter. The resulting enzyme solution was dialyzed at 4 °C against 2 L of buffer A overnight, affording the [^{3}H]PLP-reconstituted GABA-AT solution.

Inactivation of [7-^{3}H]PLP-Reconstituted GABA-AT by 17 and Cofactor Analysis. A 60 μL portion of buffer A containing [7-^{3}H]PLP-reconstituted GABA-AT (one-fifth of the amount prepared above), α-ketoglutarate (3 mM), and **17** (4 mM) was protected from light and incubated at rt overnight until the activity of GABA-AT was less than 1%. To the inactivated enzyme solution was added 1 M KOH (1 drop) to adjust the pH to 11. The mixture was allowed to stand at rt for 1 h, and then trifluoroacetic acid (TFA) (6.7 μL) was added. The mixture was allowed to stand for another 5 min, and the resulting denatured enzyme solution was centrifuged at 13400 rpm for 5 min. The supernatant was collected, and the pellet was rinsed with 2 × 50 μL of buffer A containing 10% TFA and centrifuged. The supernatant and rinses were combined and lyophilized. The resulting solid was dissolved in 100 μL of a solution containing 1 mM PLP and 1 mM PMP standards and injected into an HPLC with an Econosil C18 column (4.6 mm × 150 mm, 10 μm). Water (with 0.1% TFA)/acetonitrile (with 0.1% TFA) was used as the mobile phase (0% acetonitrile, 0.5 mL/min, 25 min; then gradient to 90% acetonitrile, 1.0 mL/min, 30 min). Under these conditions, PMP eluted at 8 min and PLP at 13 min. Fractions were collected every minute, and the radioactivity was measured by liquid scintillation counting.

Mass Spectrometric Analysis of the Inactivated GABA-AT. A 50 μL portion of ammonium bicarbonate buffer (50 mM, pH 7.4) containing GABA-AT (23 μg, 0.21 nmol), α-ketoglutarate (5 mM), and **17** (43 mM) was protected from light and incubated at rt overnight until the activity of GABA-AT was less than 1%. Another 50 μL of ammonium bicarbonate buffer (50 mM, pH 7.4) containing GABA-AT (23 μg, 0.21 nmol) and α-ketoglutarate (5 mM) was subjected to the same conditions as a control. After incubation, formic acid (10 μL) was added to each sample, and 20 μL of each resulting solution was loaded onto a 5 μm Luna C18 column (2 mm i.d.; 150 mm) (Phenomenex, Torrance, CA, USA). A 30 min LC gradient was employed at a flow rate of 200 μL/min on an Agilent 1150 LC system. Mass spectrometry was performed on a Q-Exactive mass spectrometer. Intact MS spectra were acquired at a resolution of 35000. The top five most intense ions were selected for fragmentation in a data-dependent acquisition mode. Mass spectra were acquired at a resolution of 17500.

Crystallization and Data Collection. Potassium pyrophosphate buffer (500 μL, 50 mM, pH 8.5) containing GABA-AT (200 μg, 1.82 nmol), α-ketoglutarate (5 mM), β-mercaptoethanol (5 mM), and **17** (37 mM) was protected from light and incubated at rt overnight until the activity of GABA-AT was less than 3%. The inactivated GABA-AT was then buffer-exchanged into a sodium acetate buffer (40 mM, pH 5.5) by centrifugation before the initial crystallization screening and optimization. The crystals were obtained in hanging drops comprising 1 μL of 10 mg/mL inactivated GABA-AT and 1 μL of reservoir solution containing 0.1 M ammonium acetate, 0.1 M Bis-Tris (pH 5.5), and 17% (w/v) PEG 10000. Diffraction-quality crystals grew within 4−5 days at ambient temperature. For X-ray data collection, these crystals were briefly soaked in the reservoir solution with additional 20% (v/v) glycerol as a cryoprotectant and then flash-frozen in liquid nitrogen. Crystallographic data were collected on beamlines 23ID-B and 23ID-D of GM/CA@APS of the Advanced Photon Source (APS) using X-rays with a wavelength of 0.99 Å and a Rayonix (formerly MAR-USA) 4 × 4 tiled CCD detector with a 300 mm^2 sensitive area. All of the data were indexed, integrated, and scaled with HKL2000. Data collection and processing statistics are given in Table S1 in the Supporting Information.

Phasing, Model Building, and Refinement. Molecular replacement for the inactivated GABA-AT was carried out using the program Phaser from the CCP4 software suite.[40] The tetrameric structure of native GABA-AT from pig brain was used as the starting search model, in which all solvent and PLP molecules were deleted. The initial R_{free} and R factor of the correct solution were 29.59% and 28.91%, respectively. The rigid-body refinement was followed by restrained refinement with Refmac5[41] and further manual model inspection and adjustments with Coot.[42] When the refinement converged, the $F_o - F_c$ difference maps, before incorporation of ligands into the structures, showed a well-defined electron density for both PLP and the inactivator tetrahydrothiophene (Figure 4A). The structure of the inactivator tetrahydrothiophene was built in Chemdraw (a "Mol" file); the molecule was regularized, and then the chemical restraints were generated in the program JLigand.[43] The PLP and the inactivator were fitted into the residual electron density in COOT after the rest of the structure, including most of the solvent molecules, had been refined. The R_{free} and R_{work} for inactivated GABA-AT were 20.4% and 17.2%,

DOI: 10.1021/jacs.5b01155
J. Am. Chem. Soc. 2015, 137, 4525−4533

respectively (Table S1 in the Supporting Information). All of the structural figures were made in UCSF Chimera.[44]

■ ASSOCIATED CONTENT

Supporting Information

NMR spectra, mass spectra, crystallographic data collection and processing statistics, and an overlay of in silico models of the PLP−**39** and PLP−**17** adducts. This material is available free of charge via the Internet at http://pubs.acs.org.

■ AUTHOR INFORMATION

Corresponding Author

*Agman@chem.northwestern.edu

Notes

The authors declare no competing financial interest.

■ ACKNOWLEDGMENTS

We are grateful to the National Institutes of Health for financial support (Grants GM066132 and DA030604 to R.B.S.; GM067725 to N.L.K.). GM/CA@APS has been funded in whole or in part with Federal funds from the National Cancer Institute (ACB-12002) and the National Institute of General Medical Sciences (AGM-12006). This research used resources of the Advanced Photon Source, a U.S. Department of Energy (DOE) Office of Science User Facility operated for the DOE Office of Science by Argonne National Laboratory under Contract DE-AC02-06CH11357. The authors thank Drs. Jose Juncosa and Hyunbeom Lee for helpful discussions and assistance in the purification of GABA-AT from pig brain and Dr. Boobalan Pachaiyappan for constructing the computer model of **39** docked into the enzyme using GOLD (Figure S25 in the Supporting Information). The authors also thank Park Packing Co. (Chicago, IL) for their generosity in providing fresh pig brains for this study. Support for the spectrometer funding was provided by the International Institute of Nanotechnology.

■ REFERENCES

(1) Chapter 1: Basic Mechanisms Underlying Seizures and Epilepsy. In *An Introduction to Epilepsy [Internet]*; Bromfield, E. B., Cavazos, J. E., Sirven, J. I., Eds.; American Epilepsy Society: West Hartford, CT, 2006.

(2) Epilepsy Foundation. About Epilepsy: The Basics. http://www.epilepsy.com/learn/about-epilepsy-basics (accessed July 29, 2014).

(3) Karlsson, A.; Fonnum, F.; Malthe-Sørenssen, D.; Storm-Mathisen, J. *Biochem. Pharmacol.* **1974**, *23*, 3053−3061.

(4) Baxter, C. F.; Roberts, E. *J. Biol. Chem.* **1958**, *233*, 1135−1139.

(5) Durkin, M. M.; Smith, K. E.; Borden, L. A.; Weinshank, R. L.; Branchek, T. A.; Gustafson, E. L. *Mol. Brain Res.* **1995**, *33*, 7−21.

(6) Yogeeswari, P.; Sriram, D.; Vaigundaragavendran, J. *Curr. Drug Metab.* **2005**, *6*, 127−139.

(7) Nishino, N.; Fujiwara, H.; Noguchi-Kuno, S. A.; Tanaka, C. *Jpn. J. Pharmacol.* **1988**, *48*, 331−339.

(8) Aoyagi, T.; Wada, T.; Nagai, M.; Kojima, F.; Harada, S.; Takeuchi, T.; Takahashi, H.; Hirokawa, K.; Tsumita, T. *Chem. Pharm. Bull.* **1990**, *38*, 1748−1749.

(9) Iversen, L. L.; Bird, E. D.; Mackay, A. V.; Rayner, C. N. *J. Psychiatr. Res.* **1974**, *11*, 255−256.

(10) Dewey, S. L.; Morgan, A. E.; Ashby, C. R.; Horan, B.; Kushner, S. A.; Logan, J.; Volkow, N. D.; Fowler, J. S.; Gardner, E. L.; Brodie, J. D. *Synapse* **1998**, *30*, 119−129.

(11) Gale, K. *Epilepsia* **1989**, *30* (Suppl. 3), S1−S11.

(12) Van Gelder, N. M.; Elliott, K. A. C. *J. Neurochem.* **1958**, *3*, 139−143.

(13) Singh, J.; Petter, R. C.; Baillie, T. A.; Whitty, A. *Nat. Rev. Drug Discovery* **2011**, *10*, 307−317.

(14) Lippert, B.; Metcalf, B. W.; Jung, M. J.; Casara, P. *Eur. J. Biochem.* **1977**, *74*, 441−445.

(15) Waterhouse, E. J.; Mims, K. N.; Gowda, S. N. *Neuropsychiatr. Dis. Treat.* **2009**, *5*, 505−515.

(16) Tassinari, C. A.; Michelucci, R.; Ambrosetto, G.; Salvi, F. *Arch. Neurol.* **1987**, *44*, 907−910.

(17) Browne, T. R.; Mattson, R. H.; Penry, J. K.; Smith, D. B.; Treiman, D. M.; Wilder, B. J.; Ben-Menachem, E.; Miketta, R. M.; Sherry, K. M.; Szabo, G. K. *Br. J. Clin. Pharmacol.* **1989**, *27* (Suppl. 1), 95S−100S.

(18) Sivenius, M. R.; Ylinen, A.; Murros, K.; Matilainen, R.; Riekkinen, P. *Epilepsia* **1987**, *28*, 688−692.

(19) Sander, J. W.; Hart, Y. M.; Trimble, M. R.; Shorvon, S. D. *J. Neurol. Neurosurg. Psychiatry* **1991**, *54*, 435−439.

(20) Wild, J. M.; Chiron, C.; Ahn, H.; Baulac, M.; Bursztyn, J.; Gandolfo, E.; Goldberg, I.; Goñi, F. J.; Mercier, F.; Nordmann, J.-P.; Safran, A. B.; Schiefer, U.; Perucca, E. *CNS Drugs* **2009**, *23*, 965−982.

(21) Nanavati, S. M.; Silverman, R. B. *J. Am. Chem. Soc.* **1991**, *113*, 9341−9349.

(22) Choi, S.; Storici, P.; Schirmer, T.; Silverman, R. B. *J. Am. Chem. Soc.* **2002**, *124*, 1620−1624.

(23) Pan, Y.; Qiu, J.; Silverman, R. B. *J. Med. Chem.* **2003**, *46*, 5292−5293.

(24) Okumura, H.; Omote, M.; Takeshita, S. *Arzneimittelforschung* **1996**, *46*, 459−462.

(25) Pan, Y.; Gerasimov, M. R.; Kvist, T.; Wellendorph, P.; Madsen, K. K.; Pera, E.; Lee, H.; Schousboe, A.; Chebib, M.; Bräuner-Osborne, H.; Craft, C. M.; Brodie, J. D.; Schiffer, W. K.; Dewey, S. L.; Miller, S. R.; Silverman, R. B. *J. Med. Chem.* **2012**, *55*, 357−366.

(26) Silverman, R. B. *J. Med. Chem.* **2012**, *55*, 567−575.

(27) Adams, J. L.; Chen, T. M.; Metcalf, B. W. *J. Org. Chem.* **1985**, *50*, 2730−2736.

(28) Fu, M.; Nikolic, D.; Van Breemen, R. B.; Silverman, R. B. *J. Am. Chem. Soc.* **1999**, *121*, 7751−7759.

(29) Kitz, R.; Wilson, I. B. *J. Biol. Chem.* **1962**, *237*, 3245−3249.

(30) Liu, D.; Pozharski, E.; Lepore, B. W.; Fu, M.; Silverman, R. B.; Petsko, G. A.; Ringe, D. *Biochemistry* **2007**, *46*, 10517−10527.

(31) Iwaoka, M.; Takemoto, S.; Okada, M.; Tomoda, S. *Chem. Lett.* **2001**, 132−133.

(32) Nagao, Y.; Hirata, T.; Goto, S.; Sano, S.; Kakehi, A.; Iizuka, K.; Shiro, M. *J. Am. Chem. Soc.* **1998**, *120*, 3104−3110.

(33) Ioannidis, S.; Lamb, M. L.; Almeida, L.; Guan, H.; Peng, B.; Bebernitz, G.; Bell, K.; Alimzhanov, M.; Zinda, M. *Bioorg. Med. Chem. Lett.* **2010**, *20*, 1669−1673.

(34) Iwaoka, M.; Takemoto, S.; Tomoda, S. *J. Am. Chem. Soc.* **2002**, *124*, 10613−10620.

(35) Jones, G.; Willett, P.; Glen, R. C. *J. Mol. Biol.* **1995**, *245*, 43−53.

(36) Evans, C.; McCague, R.; Roberts, S. M.; Sutherland, A. G. *J. Chem. Soc., Perkin Trans. 1* **1991**, 656−657.

(37) Forró, E.; Fülöp, F. *Eur. J. Org. Chem.* **2008**, 5263−5268.

(38) Koo, Y. K.; Nandi, D.; Silverman, R. B. *Arch. Biochem. Biophys.* **2000**, *374*, 248−254.

(39) Yung-Chi, C.; Prusoff, W. H. *Biochem. Pharmacol.* **1973**, *22*, 3099−3108.

(40) Collaborative Computational Project Number 4 *Acta Crystallogr., Sect. D* **1994**, *50*, 760−763.

(41) Emsley, P.; Cowtan, K. *Acta Crystallogr., Sect. D* **2004**, *60*, 2126−2132.

(42) Murshudov, G. N.; Vagin, A. A.; Dodson, E. J. *Acta Crystallogr., Sect. D* **1997**, *53*, 240−255.

(43) Lebedev, A. A.; Young, P.; Isupov, M. N.; Moroz, O. V.; Vagin, A. A.; Murshudov, G. N. *Acta Crystallogr., Sect. D* **2012**, *68*, 431−440.

(44) Pettersen, E. F.; Goddard, T. D.; Huang, C. C.; Couch, G. S.; Greenblatt, D. M.; Meng, E. C.; Ferrin, T. E. *J. Comput. Chem.* **2004**, *25*, 1605−1612.

DOI: 10.1021/jacs.5b01155
J. Am. Chem. Soc. 2015, 137, 4525−4533